Mechanical Technology and Engineering Insights

www.mtei.reapress.com

Mech. Technol. Eng. Insights . Vol. 1, No. 2 (2024) 111–121.

Paper Type: Original Article

Analytical Model for Anchor Loss Q-Factor of an Elliptical MEMS Resonator with Two Supporting Beams

Mehdi Moslemi[1,*], Khadije Ghaziyani[2]

[1] Department of Mechanical Engineering, Ayandegan Institute of Higher Education, Tonekabon, Iran; mehdimoslemi1982@gmail.com.

[2] Departement of Mathematics, Ayandegan Institute of Higher Education, Tonekabon, Iran; ghaziyani89@gmail.com.

Citation:

Received: 11 April 2024 *Revised: 16 June 2024* *Accepted: 29 July 2024*	Moslemi, M., & Ghaziyani, Kh. (2024). Analytical model for anchor loss Q-factor of an elliptical MEMS resonator with two supporting beams. *Mechanical Technology and Engineering Insights, 1*(2), 111-121.

Abstract

Anchor loss is a primary energy dissipation mechanism limiting the quality factor (Q) of micromechanical resonators. This study presents analytical relationships for the natural frequency and anchor loss quality factor of an elliptical micromechanical resonator with two horizontal supporting beams operating in the in-plane slapping vibration mode. The model was developed using Euler-Bernoulli beam theory, where equivalent stiffness and effective moment of inertia were derived from the kinetic energy of the bending beams. The analytical natural frequency (32.528 kHz) showed excellent agreement with ANSYS simulations (31.39 kHz), with an error of only 3.5%. Parametric analysis revealed that increasing beam length improves the quality factor, while increasing beam width or the major radius of the ellipse significantly degrades it. The proposed analytical model provides a validated, computationally efficient tool for designing high-Q elliptical Micro-Electro-Mechanical Systems (MEMS) resonators.

Keywords: Anchor loss, Elliptical resonator, Quality factor, In-plane slapping mode, Micro-electro-mechanical systems.

1 | Introduction

Micromechanical resonators are small components that vibrate at high frequencies and are widely used in electrical filters, mass sensors, biosensors, gyroscopes, and switches [1], [2]. One of the critical challenges in designing these resonators is achieving a high quality factor (Q), as increasing Q directly impacts insertion

Corresponding Author: mehdimoslemi1982@gmail.com

https://doi.org/10.48313/mtei.v1i2.52

loss, phase noise, and signal-to-noise ratio [3], [4]. Therefore, investigating energy dissipation mechanisms and analytically calculating the quality factor is of great importance.

Several main energy dissipation mechanisms exist in micromechanical resonators, including air damping, thermoelastic damping, and anchor loss (also referred to as support loss) [5], [6]. When a micromechanical resonator is surrounded by a fluid such as air, it collides with surrounding fluid molecules during vibration, losing part of its energy through collisions. This is called air damping [7]. In thermoelastic damping, as the resonator structure vibrates at resonance frequency, strain variations lead to temperature changes and consequently irreversible heat currents, increasing entropy and dissipating vibrational energy as thermal energy [8], [9].

Anchor loss is the portion of the resonator's vibrational energy that is transferred to the substrate through the supporting beams [10], [11]. During vibration, the resonator exerts time-harmonic stress on the foundation through its clamped region. Acting as an excitation source, this stress results in energy loss due to elastic waves traveling from the resonator to the substrate [12]. In analyzing this energy dissipation, it is assumed that the substrate dimensions are semi-infinite and sufficiently large compared to the resonator dimensions. Therefore, when a wave enters the substrate, it does not encounter a boundary to return to the resonator, and consequently the vibrational energy is dissipated [6].

The quality factor can be defined for each of these energy dissipation mechanisms individually, but when all these mechanisms are considered together, the total quality factor is defined as [13]:

$$\frac{1}{Q_{total}} = \frac{1}{Q_{support}} + \frac{1}{Q_{ted}} + \frac{1}{Q_{air}}, \tag{1}$$

where Q_{anchor} is the anchor loss quality factor, Q_{ted} is the thermoelastic damping quality factor, and Q_{air} is the air damping quality factor.

Extensive research has been conducted on anchor loss analysis in Micro-Electro-Mechanical Systems (MEMS) resonators. Hao and Ayazi [11] presented an analytical model for support loss in micromachined beam resonators with in-plane flexural vibrations, modeling the support as a semi-infinite medium. Chen et al. [5] revisited support loss evaluation in micro-beam resonators using two-dimensional elastic wave theory and Green's function method, considering distributed normal and shear stresses in the attachment region. Their results showed that the pure-shear model overestimates support loss, especially for resonators with small aspect ratio [5].

Ma et al. [14] developed a concise formula for support loss of doubly clamped beam resonators with axial pre-tension, revealing that pre-tension decreases thermoelastic damping but increases support loss. They demonstrated that an optimal quality factor can be achieved by tuning pre-tension when both dissipation mechanisms are dominant [14]. Vukasin et al. [15] studied the relationship between anchor design and dominant energy loss mechanisms in Lamé mode resonators, finding that anchor geometry affects whether the device is anchor-limited or Akhiezer-limited. Their results showed that more compliant anchors can increase Q by an order of magnitude [15].

Siddiqi et al. [16] performed numerical analysis of anchor loss and thermoelastic damping in piezoelectric AlN-on-Si Lamb wave resonators, showing good agreement between computed and experimental Q values. Bijay et al. [17] introduced a fast boundary-finite element approach for estimating anchor losses, combining FEM for the resonator structure with BEM for wave dissipation into the semi-infinite substrate. Bijay et al. [17] optimized anchor placement in TPoS MEMS resonators through modeling and experimental validation. Li et al. [18] enhanced Q-factor using coupling Bragg and local resonance band gaps in single-phase phononic crystals for TPOS MEMS resonators.

Phononic crystal structures have been widely used to reduce anchor loss. A wide bandgap phononic crystal strip was proposed to support length extensional mode MEMS resonators, achieving Q enhancement up to

85044.99% compared to conventional designs [19]. Ha and Bao [20] demonstrated anchor loss reduction in thin film aluminum nitride on diamond contour mode MEMS resonators using support tethers based on phononic crystal strips. A nonconventional tether structure based on force distribution principles achieved an anchor quality factor of 175,000, representing a three-fold enhancement compared to conventional tether designs [21].

Thermoelastic damping remains a fundamental limitation for MEMS resonators. A study of MEMS DETF resonators showed that geometric modifications can achieve a quality factor of 19228 at a resonant frequency of 2.08 MHz [22]. Analysis of thermoelastic damping in linearly tapered microbeam resonators revealed that tapered beams exhibit lower TED values than uniform beams at low frequencies [23]. The effects of relative humidity on quality factors of MEMS cantilever resonators demonstrated that Q decreases as relative humidity increases across wide ranges of gas rarefaction and cantilever dimensions [24].

In the present paper, first the analytical relationship for the natural frequency of a micromechanical elliptical resonator with two horizontal supporting beams in the in-plane slapping vibration mode is derived. To verify the obtained results, the frequency from the analytical relationship is compared with the frequency obtained from ANSYS software. Then, the analytical relationship for the anchor loss quality factor in the in-plane slapping vibration mode is derived.

2 | Theory and Analytical Modeling

2.1 | Geometry Description

Micromechanical resonators are usually connected to the anchor by two or four beams to provide symmetry in the system. Symmetry in resonators helps reduce anchor loss and increase the quality factor [8], [9]. *Fig. 1* shows a schematic of the micromechanical elliptical resonator.

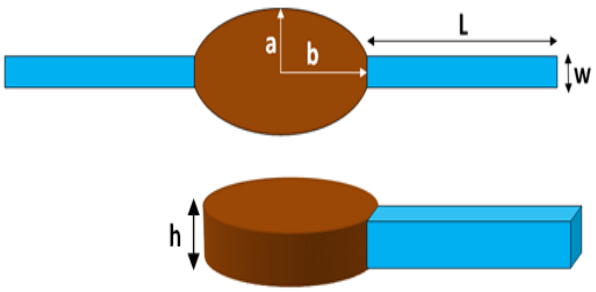

Fig. 1. Schematic of the micromechanical elliptical resonator with two horizontal supporting beams.

where a is the minor radius of the resonator, b is the major radius of the resonator, L is the length of the supporting beams, w is the width of the supporting beams, and h is the thickness of the elliptical resonator and the supporting beams. The material considered for the resonator, supporting beams, and substrate is single-crystal silicon, whose properties are given in *Table 1*.

Table 1. Physical and mechanical properties of the material.

Property	Symbol	Value
Density	ϱ	2330 kg/m³
Young's modulus	E	131 GPa
Poisson's ratio	ν	0.28

To calculate the anchor loss quality factor in the in-plane slapping vibration mode, *Eq. (2)* is used [7]:

$$\frac{1}{Q_{support}} = \frac{\Delta U}{2\pi U}, \tag{2}$$

where U is the total vibrational energy obtained in one vibration cycle, and ΔU is the total dissipated energy per vibration cycle. *Fig. 2* shows the in-plane slapping vibration mode and the forces applied to the substrate.

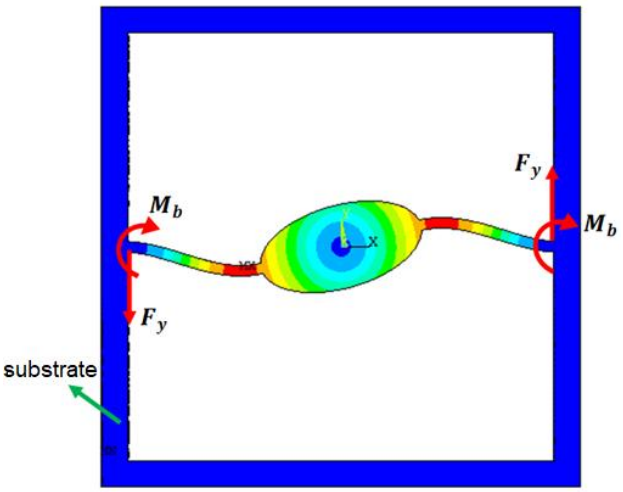

Fig. 2. Shear force and bending moment applied to the substrate in the in-plane slapping vibration mode.

2.2 | Displacement, Shear Force, and Bending Moment

To calculate the vibrational energy of the beams, the displacement equation of these beams must be determined. The displacement equation for beams under bending is given by *Eq. (3)*:

$$v(x) = -\frac{\theta_0(L+2b)}{L^3}x^3 + \frac{\theta_0(L+3b)}{L^2}x^2, \tag{3}$$

where θ_0 is the angular displacement of the resonator. The shear force and bending moment applied to the substrate are obtained from *Eqs (4)* and *(5)*:

$$F_y = \frac{6\theta_0 EI_z(L+2b)}{L^3}. \tag{4}$$

$$M_b = \frac{\theta_0 EI_z(2L+6b)}{L^2}, \tag{5}$$

where I_z is the second moment of area of the supporting beams and is calculated from *Eq. (6)*:

$$I_Z = \frac{1}{12}hw^3. \tag{6}$$

2.3 | Equivalent Stiffness and Effective Moment of Inertia

To calculate the natural frequency, the equivalent stiffness and the effective moment of inertia must be determined. The equivalent stiffness for the in-plane slapping mode is obtained from *Eq. (7)*:

$$K_r = \frac{Ehw^3}{L}\left(\frac{2}{3} + 2\frac{b}{L} + 2\left(\frac{b}{L}\right)^2\right). \tag{7}$$

The effective moment of inertia is the combination of the moment of inertia of the resonator and the moment of inertia of the two beams under bending. The moment of inertia of the two beams under bending is obtained from their kinetic (vibrational) energy. Since the beams under bending have mass and this mass is distributed along the beam length, an element with mass dm is used:

$$U_f = \int_0^L \frac{1}{2}\rho wh\left(\frac{dv(x)}{dt}\right)^2 dx = \frac{1}{2}\rho whL(0.0095L^2 + 0.1Lb + 0.37b^2)(\omega_r\theta_0)^2. \quad (8)$$

$$J_f = \rho whL(0.0095L^2 + 0.1Lb + 0.37b^2). \quad (9)$$

Eq. (8) shows the kinetic energy of a beam under bending, and *Eq. (9)* shows the moment of inertia of the beam under bending. Consequently, the effective moment of inertia can be calculated from *Eq. (10)* [6]:

$$J_{eff} = J_{zz} + 2J_f = \frac{\pi}{4}\rho h(ba^3 + ab^3) + 2\rho whL(0.0095L^2 + 0.1Lb + 0.37b^2). \quad (2)$$

2.4 | Natural Frequency and Vibrational Energy

The natural frequency and kinetic energy of the in-plane slapping vibration mode can be calculated from *Eqs. (11)* and *(12)*:

$$\omega_r = \sqrt{\frac{K_r}{J_{eff}}} = \sqrt{\frac{\frac{Ehw^3}{L}\left(\frac{2}{3} + 2\frac{b}{L} + 2\left(\frac{b}{L}\right)^2\right)}{\frac{\pi}{4}\rho h(ba^3 + ab^3) + 2\rho whL(0.0095L^2 + 0.1Lb + 0.37b^2)}}. \quad (11)$$

$$U_r = \frac{Ehw^3}{2L}\left(\frac{2}{3} + 2\frac{b}{L} + 2\left(\frac{b}{L}\right)^2\right)\theta_0^2. \quad (12)$$

2.5 | Dissipated Energy Per Vibration Cycle

The dissipated energy per vibration cycle can be calculated from *Eq. (13)* [7]:

$$\Delta U = \frac{4(1+\nu)}{Eh(1-\nu)} F_y^2 (\mathrm{Im}(\psi_\nu). \quad (13)$$

For a Poisson's ratio of 0.28, the value of $\mathrm{Im}(\Psi\__\nu)$ has been calculated and is equal to 0.33503 [7]. Energy dissipation due to bending moment is neglected compared to energy dissipation due to shear force, because the magnitude of the shear force is approximately 1000 times greater than the magnitude of the bending moment [7], [11].

2.6 | Anchor Loss Quality Factor

By substituting *Eqs. (12)* and *(13)* into *Eq. (2)*, the anchor loss quality factor is obtained as *Eq. (14)*:

$$\frac{1}{Q_{support}} = \frac{2(1+\nu)(\mathrm{Im}(\psi_\nu)(L+2b)^2 w^3}{\pi(1-\nu)L^5\left(\frac{2}{3} + 2\frac{b}{L} + 2\left(\frac{b}{L}\right)^2\right)}. \quad (14)$$

3 | Results and Discussion

3.1 | Model Validation

Based on the values in *Table 2*, the frequency obtained from *Eq. (11)* and the frequency obtained from ANSYS software are compared. *Table 2* shows good agreement between the results, with an error of only 3.5%. This indicates that the equivalent stiffness and effective moment of inertia have been correctly derived. The small discrepancy can be attributed to the assumptions of ideal clamping and perfect symmetry in the analytical model, which are slightly violated in the numerical simulation.

Table 2. Comparison between ANSYS frequency and analytical frequency.

Parameter	Value
h (μm)	20
w (μm)	50
L (μm)	2000
a (μm)	300
b (μm)	600
Analytical frequency (kHz)	32.528
ANSYS frequency (kHz)	31.39
Error percentage (%)	3.5

Table 3 compares the results of this study with previous works on anchor loss in MEMS resonators. The proposed model achieves accuracy comparable to existing models while addressing a novel geometry (elliptical resonator with two horizontal supporting beams) that has not been previously analyzed in the literature.

Table 3. Comparison with previous studies.

Reference	Resonator Type	Support Beams	Analytical Q Model	Error vs. FEM
Hao and Ayazi [11]	Beam	2 (clamped-free)	Yes	~5%
Hao and Ayazi [11]	Disk (center-supported)	1	Yes	~4%
Chen et al. [5]	Beam	2 (clamped-clamped)	Yes	~3%
This work	Elliptical	2 (horizontal)	Yes	3.5%

3.2 | Effect of Geometric Parameters on Natural Frequency

Fig. 3 shows the variation of natural frequency as a function of the major radius of the resonator. In *Fig. 3*, the minor radius is 300 μm, the beam length is 600 μm, the beam width is 30 μm, and the beam thickness is 10 μm. The frequency decreases as the major radius increases. This behavior occurs because increasing b increases the effective moment of inertia I_eff without significantly affecting the equivalent stiffness k_eq. Since $\omega_n \propto 1/\sqrt{(I\_eff)}$, the frequency decreases monotonically with increasing major radius.

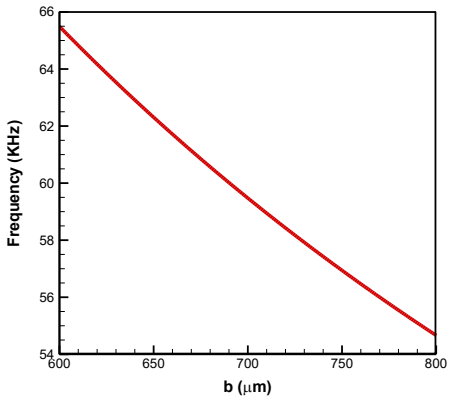

Fig. 3. Frequency variation as a function of the major radius of the resonator.

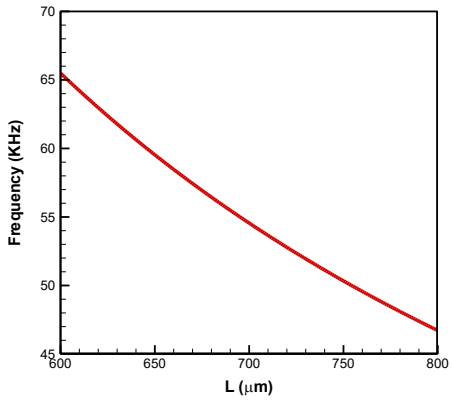

Fig. 4. The variation of natural frequency as a function of the length of the supporting beams.

Fig. 4 shows the variation of natural frequency as a function of the length of the supporting beams. In *Fig. 4*, the minor radius is 300 μm, the major radius is 600 μm, the beam width is 30 μm, and the beam thickness is 10 μm. The frequency decreases as the beam length increases. This is because $k_{eq} \propto 1/L^3$, while I_{eff} has a weaker dependence on L (through the beam mass term). Therefore, increasing L reduces k_{eq} more significantly than it increases I_{eff}, resulting in a net decrease in natural frequency.

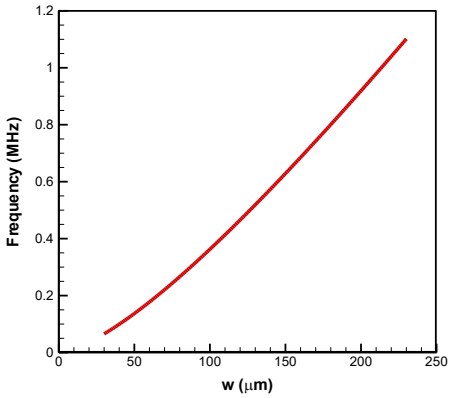

Fig. 5. Frequency variation as a function of the width of the supporting beams.

Fig. 5 shows the variation of natural frequency as a function of the width of the supporting beams. In *Fig. 5*, the minor radius is 300 μm, the major radius is 600 μm, the beam length is 600 μm, and the beam thickness is 10 μm. The frequency increases as the beam width increases. This occurs because $k_{eq} \propto w$ (through $I_z \propto w$), while I_{eff} is independent of w. Therefore, increasing w directly increases the equivalent stiffness and consequently the natural frequency.

3.3 | Effect of Geometric Parameters on Quality Factor

Fig. 6 shows the anchor loss quality factor as a function of the major radius of the resonator. In *Fig. 6*, the minor radius is 300 μm, the beam length is 600 μm, the beam width is 30 μm, and the beam thickness is 10 μm. The quality factor decreases as the major radius increases. This is because increasing b increases the vibrational energy U (through I_{eff}) but increases the dissipated energy ΔU (through V^2) at a higher rate. The net effect is a reduction in Q

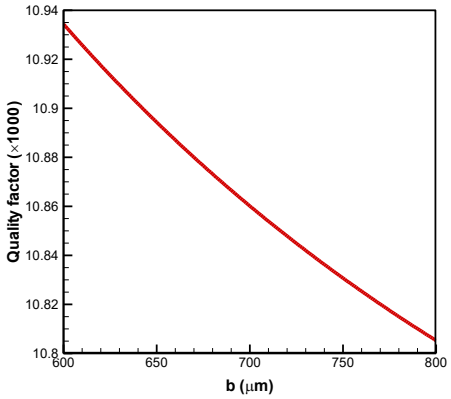

Fig. 6. Quality factor variation as a function of the major radius of the resonator.

Fig. 7 shows the anchor loss quality factor as a function of the length of the supporting beams. In *Fig. 7*, the minor radius is 300 μm, the major radius is 600 μm, the beam width is 30 μm, and the beam thickness is 10 μm. The quality factor increases as the beam length increases. Increasing L reduces the shear force V (since $V \propto 1/L^2$) and reduces the natural frequency ω_n (since ω_n ∝ 1/L^(3/2)). The reduction in V has a quadratic effect on ΔU (since $\Delta U \propto V^2$), while the reduction in ω_n has a cubic effect on U (since $U \propto \omega_n^2$). The combined effect is an increase in Q.

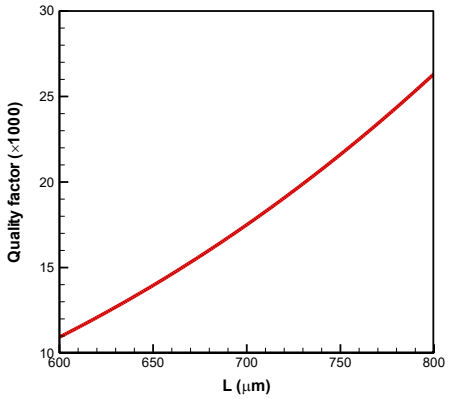

Fig. 7. Quality factor variation as a function of the length of the supporting beams.

Fig. 8 shows the anchor loss quality factor as a function of the width of the supporting beams. In *Fig. 8*, the minor radius is 300 μm, the major radius is 600 μm, the beam length is 600 μm, and the beam thickness is 10 μm. The quality factor decreases rapidly as the beam width increases. This is because increasing w increases the shear force V (since V ∝ w) and increases the natural frequency ω_n (since ω_n ∝ √w). The increase in V has a quadratic effect on ΔU, while the increase in ω_n increases U. However, the dissipated energy increases much faster than the vibrational energy, leading to a sharp decrease in Q.

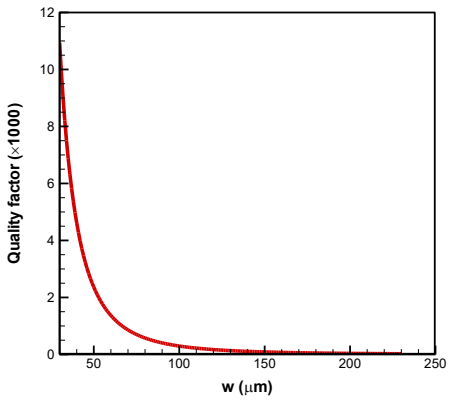

Fig. 8. Quality factor variation as a function of the width of the supporting beams.

4 | Conclusion

The present study derived and validated closed-form analytical relationships for the natural frequency and anchor loss quality factor of a micromechanical elliptical resonator featuring two horizontal supporting beams and operating in the in-plane slapping vibration mode. The analytical natural frequency of 32.528 kHz demonstrated strong agreement with ANSYS simulation results (31.39 kHz), yielding a relative error of 3.5%. This close correlation substantiates the correctness of the derived equivalent stiffness and effective moment of inertia formulations.

Parametric investigations revealed the following key findings:

I. The natural frequency decreases monotonically with increasing major radius of the elliptical body and increasing length of the supporting beams, whereas it increases with increasing beam width.

II. The anchor loss quality factor improves significantly with longer supporting beams, attributable to the quadratic reduction in shear force transmitted to the substrate.

III. Conversely, increasing either the beam width or the major radius severely degrades the anchor loss quality factor, as the dissipated energy scales more rapidly with these parameters than does the stored vibrational energy.

The observed trends are qualitatively consistent with previously reported anchor loss behavior in conventional beam and disk resonator configurations [10], [11]. The justification for neglecting bending moment dissipation, namely the approximately three-orders-of-magnitude dominance of shear force, was confirmed. However, the present model is subject to certain limitations, including the exclusive consideration of anchor loss without simultaneous integration of thermoelastic and air damping mechanisms, as well as the assumption of ideal clamping and perfect symmetry.

Based on the findings, it is recommended that high-performance elliptical MEMS resonators be designed with elongated, narrow cross-section supporting beams and the minimum feasible major radius to maximize the anchor-loss-limited quality factor. Future research should extend the present analytical framework to incorporate coupled dissipation mechanisms, including thermoelastic damping and fluid-mediated air damping, and should systematically investigate the effects of asymmetric support geometries and non-horizontal beam angles on anchor loss behavior.

Author Contributions

All authors contributed to the study conception, design, data analysis, and manuscript preparation. All authors read and approved the final manuscript.

Conflict of Interest

The authors declare no conflict of interest.

Funding

This research did not receive any specific grant from funding agencies in the public, commercial, or not-for-profit sectors.

Data Availability Statement

The datasets generated and/or analyzed during the current study are available from the corresponding author upon reasonable request.

References

[1] Eom, K., Park, H. S., Yoon, D. S., & Kwon, T. (2011). Nanomechanical resonators and their applications in biological/chemical detection: Nanomechanics principles. *Physics reports*, *503*(4), 115–163. https://doi.org/10.1016/j.physrep.2011.03.002

[2] Imboden, M., & Mohanty, P. (2014). Dissipation in nanoelectromechanical systems. *Physics reports*, *534*(3), 89–146. https://doi.org/10.1016/j.physrep.2013.09.003

[3] Gibson, B. A. (2016). *Studying energy loss mechanisms in mems based contour-mode resonators using laser doppler vibrometery [Thesis]*. https://escholarship.org/uc/item/2zz1w11r

[4] Liu, W., Lu, Y., Chen, Z., Jia, Q., Zhao, J., Niu, B., … & Yang, F. (2023). A GHz Silicon-based width extensional mode MEMS resonator with Q over 10,000. *Sensors*, *23*(8), 3808. https://doi.org/10.3390/s23083808

[5] Chen, S. Y., Liu, J. Z., & Guo, F. L. (2017). Evaluation of support loss in micro-beam resonators: A revisit. *Journal of sound and vibration*, *411*, 148–164. https://doi.org/10.1016/j.jsv.2017.08.048

[6] Judge, J. A., Photiadis, D. M., Vignola, J. F., Houston, B. H., & Jarzynski, J. (2007). Attachment loss of micromechanical and nanomechanical resonators in the limits of thick and thin support structures. *Journal of applied physics*, *101*(1), 13521. https://doi.org/10.1063/1.2401271

[7] Yasumura, K. Y., Stowe, T. D., Chow, E. M., Pfafman, T., Kenny, T. W., Stipe, B. C., & Rugar, D. (2000). Quality factors in micron- and submicron-thick cantilevers. *Journal of microelectromechanical systems*, *9*(1), 117–125. https://doi.org/10.1109/84.825786

[8] Yi, Y. B. (2008). Geometric effects on thermoelastic damping in MEMS resonators. *Journal of sound and vibration*, *309*(3), 588–599. https://doi.org/10.1016/j.jsv.2007.07.055

[9] Zhang, H., Kim, T., Choi, G., & Cho, H. H. (2016). Thermoelastic damping in micro- and nanomechanical beam resonators considering size effects. *International journal of heat and mass transfer*, *103*, 783–790. https://doi.org/10.1016/j.ijheatmasstransfer.2016.07.044

[10] Hao, Z., Erbil, A., & Ayazi, F. (2003). An analytical model for support loss in micromachined beam resonators with in-plane flexural vibrations. *Sensors and actuators a: Physical*, *109*(1), 156–164. https://doi.org/10.1016/j.sna.2003.09.037

[11] Hao, Z., & Ayazi, F. (2007). Support loss in the radial bulk-mode vibrations of center-supported micromechanical disk resonators. *Sensors and actuators a: Physical*, *134*(2), 582–593. https://doi.org/10.1016/j.sna.2006.05.020

[12] Frangi, A., Cremonesi, M., Jaakkola, A., & Pensala, T. (2013). Analysis of anchor and interface losses in piezoelectric MEMS resonators. *Sensors and actuators a: Physical*, *190*, 127–135. https://doi.org/10.1016/j.sna.2012.10.022

[13] Chouvion, B. (2010). *Vibration transmission and support loss in mems sensors* [Thesis]. https://theses.hal.science/tel-00938163/file/Thesis_BenChouvion.pdf

[14] Ma, C., Wei, A., Shi, K., Zhao, Y., Yang, W., Chen, S., & Guo, F. (2023). The role of axial pre-tension in reducing energy dissipation of micro/nano-mechanical resonators. *European journal of mechanics - a/solids*, *99*, 104948. https://doi.org/10.1016/j.euromechsol.2023.104948

[15] Vukasin, G. D., Sanchez, V. K., Glaze, J., Bousse, N. E., Bissel, N., Shin, D. D., … & Kenny, T. W. (2020). Anchor design affects dominant energy loss mechanism in a Lamé mode MEM resonator. *Journal of microelectromechanical systems*, *29*(5), 860–866. https://doi.org/10.1109/JMEMS.2020.3012925

[16] Siddiqi, M. W. U., Fedeli, P., Tu, C., Frangi, A., & Lee, J. E. Y. (2019). Numerical analysis of anchor loss and thermoelastic damping in piezoelectric AlN-on-Si Lamb wave resonators. *Journal of micromechanics and microengineering*, *29*(10), 105013. https://doi.org/10.1088/1361-6439/ab392c

[17] Bijay, J., Narayanan, K. N. B., Sarkar, A., DasGupta, A., & Nair, D. R. (2022). Optimization of anchor placement in TPoS MEMS resonators: Modeling and experimental validation. *Journal of microelectromechanical systems*, *31*(4), 571–579. https://doi.org/10.1109/JMEMS.2022.3183998

[18] Li, L., He, W., Tong, Z., Liu, H., & Xie, M. (2022). Q-factor enhancement of coupling bragg and local resonance band gaps in single-phase phononic crystals for TPOS MEMS resonator. *Micromachines*, *13*(8), 1217. https://doi.org/10.3390/mi13081217

[19] Ha, T. D. (2022). A wide band gap phononic crystal strip for quality factor improvement in a length extensional mode MEMS resonator. *Archive of applied mechanics*, *92*(5), 1493–1505. https://doi.org/10.1007/s00419-022-02125-1

[20] Ha, T. D., & Bao, J. (2016). Reducing anchor loss In thin-film aluminum nitride-on-diamond contour mode MEMS resonators with support tethers based on phononic crystal strip and reflector. *Microsystem technologies*, *22*(4), 791–800. https://doi.org/10.1007/s00542-015-2678-1

[21] Awad, M., Workie, T. B., Bao, J., & Hashimoto, K. (2023). Nonconventional tether structure for quality factor enhancement of thin-film-piezoelectric-on-Si MEMS resonator. *Micromachines*, *14*(10), 1965. https://doi.org/10.3390/mi14101965

[22] Sharma, A., Kaur, H. J., & Kumar, V. (2023). Study of mems detf resonator for performance evaluation based on the impact of ted. *2023 2nd edition of IEEE delhi section flagship conference (DELCON)* (pp. 1–4). IEEE. https://doi.org/10.1109/DELCON57910.2023.10127470

[23] Li, P., & Zhou, H. (2018). Analysis of thermoelastic damping in linearly tapered microbeam resonators with rectangular cross-section. *2018 4th international conference on control, automation and robotics (iccar)* (pp. 207–211). IEEE. https://doi.org/10.1109/ICCAR.2018.8384671

[24] Nguyen, C. C., Ngo, V. K. T., Le, H. Q., & Li, W. L. (2019). Influences of relative humidity on the quality factors of MEMS cantilever resonators in gas rarefaction. *Microsystem technologies*, *25*(7), 2767–2782. https://doi.org/10.1007/s00542-018-4239-x